Washington University School of Medicine
Digital Commons@Becker

Open Access Publications

2013

AhrC and Eep are biofilm infection-associated virulence factors in enterococcus faecalis

Kristi L. Frank
University of Minnesota - Twin Cities

Pascale S. Guiton
Washington University School of Medicine in St. Louis

Aaron M T Barnes
University of Minnesota - Twin Cities

Dawn A. Manlas
University of Minnesota - Twin Cities

Olivia N. Chuang-Smith
University of Minnesota - Twin Cities

See next page for additional authors

Follow this and additional works at: http://digitalcommons.wustl.edu/open_access_pubs

Authors

Kristi L. Frank, Pascale S. Guiton, Aaron M T Barnes, Dawn A. Manlas, Olivia N. Chuang-Smith, Petra L. Kohler, Adam R. Spaulding, Scott J. Hultgren, Patrick M. Schievert, and Gary M. Dunny

Infection and Immunity

AhrC and Eep Are Biofilm Infection-Associated Virulence Factors in Enterococcus faecalis

Kristi L. Frank, Pascale S. Guiton, Aaron M. T. Barnes,
Dawn A. Manias, Olivia N. Chuang-Smith, Petra L. Kohler,
Adam R. Spaulding, Scott J. Hultgren, Patrick M. Schlievert
and Gary M. Dunny

Updated information and services can be found at:
http://iai.asm.org/content/81/5/1696

These include:

REFERENCES
This article cites 56 articles, 28 of which can be accessed free
at: http://iai.asm.org/content/81/5/1696#ref-list-1

CONTENT ALERTS
Receive: RSS Feeds, eTOCs, free email alerts (when new
articles cite this article), more»

Information about commercial reprint orders: **http://journals.asm.org/site/misc/reprints.xhtml**
To subscribe to to another ASM Journal go to: **http://journals.asm.org/site/subscriptions/**

AhrC and Eep Are Biofilm Infection-Associated Virulence Factors in *Enterococcus faecalis*

Kristi L. Frank,[a] Pascale S. Guiton,[b]* Aaron M. T. Barnes,[a] Dawn A. Manias,[a] Olivia N. Chuang-Smith,[a]* Petra L. Kohler,[a]* Adam R. Spaulding,[a]* Scott J. Hultgren,[b] Patrick M. Schlievert,[a]* Gary M. Dunny[a]

Department of Microbiology, University of Minnesota Medical School, Minneapolis, Minnesota, USA[a]; Department of Molecular Microbiology and Microbial Pathogenesis, Washington University School of Medicine, St. Louis, Missouri, USA[b]

Enterococcus faecalis is part of the human intestinal microbiome and is a prominent cause of health care-associated infections. The pathogenesis of many *E. faecalis* infections, including endocarditis and catheter-associated urinary tract infection (CAUTI), is related to the ability of clinical isolates to form biofilms. To identify chromosomal genetic determinants responsible for *E. faecalis* biofilm-mediated infection, we used a rabbit model of endocarditis to test strains with transposon insertions or in-frame deletions in biofilm-associated loci: *ahrC*, *argR*, *atlA*, *opuBC*, *pyrC*, *recN*, and *sepF*. Only the *ahrC* mutant was significantly attenuated in endocarditis. We demonstrate that the transcriptional regulator AhrC and the protease Eep, which we showed previously to be an endocarditis virulence factor, are also required for full virulence in murine CAUTI. Therefore, AhrC and Eep can be classified as enterococcal biofilm-associated virulence factors. Loss of *ahrC* caused defects in early attachment and accumulation of biofilm biomass. Characterization of *ahrC* transcription revealed that the temporal expression of this locus observed in wild-type cells promotes initiation of early biofilm formation and the establishment of endocarditis. This is the first report of AhrC serving as a virulence factor in any bacterial species.

The role of biofilms in the pathogenesis of infectious diseases has received significant attention over the past decade (1, 2). Microbial biofilm infections are the result of a complex interplay between surface-associated microbes embedded in an extracellular matrix and attempts by the host immune defenses to clear these often chronic infections (3). Biofilm infections occur throughout the human body on both native and implanted prosthetic surfaces (4). Animal models to study biofilm infections experimentally are as abundant as the types of infections and the bacteria that cause them (5). Likewise, the plethora of experimental approaches used to define the genetic determinants of biofilm formation in pathogenic bacteria with *in vitro* assays are too numerous to cite here. There remains, however, a paucity of knowledge on the relationship between the genetic basis of *in vitro* biofilm formation and virulence in biofilm infections.

Enterococcus faecalis, a Gram-positive constituent of the human intestinal microbiome, has become a prominent pathogen of health care-associated infections (HAIs) over the past 3 decades. Between 1980 and 2008, the frequency of HAIs caused by *E. faecalis* and *Enterococcus faecium*, the other frequently encountered enterococcal pathogen, increased by 8.8% (6). *E. faecalis* and *E. faecium* infections together accounted for 16.0% of central line-associated bloodstream HAIs, 14.9% of catheter-associated urinary tract HAIs, and 11.2% of surgical site HAIs reported to the United States National Healthcare Safety Network in 2006 and 2007 (7). *E. faecalis* is also the primary causative agent of enterococcal endocarditis (8, 9), an infection of the heart valves, which is the second leading cause of infective endocarditis in North America and the fourth worldwide (10). Enterococcal endocarditis is more prevalent than nonenterococcal endocarditis in cancer patients and is associated with an overall mortality rate of 11 to 22% (8, 9).

Biofilm formation on the surfaces of medically implantable prosthetic devices (e.g., central lines and urinary catheters) or host tissues (e.g., damaged heart valves) underlies the pathogenesis of most enterococcal infections (11). Established animal models of endocarditis and urinary tract infection (UTI), which both manifest from biofilm etiologies, have been used to study *E. faecalis* virulence (12–16). *E. faecalis* has multiple surface proteins, such as Ebp pili and Ace, that act as adhesins to bind to host cells and proteins, which resultantly promotes *in vitro* biofilm formation and virulence in models of endocarditis and UTI (11). Recently, we reported that Eep, an intramembrane protease, is also an endocarditis virulence factor (13). While an *eep* in-frame deletion mutant can attach to surfaces and form biofilms *in vitro*, we showed that early stage biofilms formed by this strain have an altered cell distribution phenotype. We further demonstrated that the endocarditis attenuation phenotype could be successfully complemented *in vivo* by expression of *eep* from a plasmid that was lost from the majority of bacteria during the course of the experimental infection. These data support the hypothesis that Eep is also important during early heart valve infection (13). However, the contribution of Eep to other biofilm infections and its function in enterococcal pathogenesis remain unknown.

E. faecalis OG1RF is a well-characterized strain that has dem-

onstrated virulence in animal models despite lacking the plasmids and mobile genetic elements known to harbor classical enterococcal virulence factors and antibiotic resistance genes (17, 18). Conserved genes in OG1RF are likely to be present in the genomes of other pathogenic *E. faecalis* strains (19), which makes the strain particularly useful for studying the biological contributions of chromosomal genes in the absence of extraneous chromosomal or extrachromosomal genetic elements. Our group previously screened an OG1RF random mini-*mariner* transposon insertion library containing approximately 15,000 clones to identify genetic determinants in the *E. faecalis* core genome that are necessary for biofilm formation in a standard microtiter plate biofilm assay (20). Ten distinct biofilm-associated loci were identified from 25 biofilm-defective transposon insertion mutants. Of these, *srtA*, coding for the housekeeping sortase, and the *ebp* pilus genes and their associated sortase gene, *srtC*, have also been implicated in enterococcal virulence (12, 16, 21, 22). In contrast, disruption of the major autolysin gene (*atlA*), an important mediator of DNA release during biofilm formation *in vitro* (23), did not result in reduced virulence in either peritonitis (24) or catheter-associated urinary tract infection (12). To the best of our knowledge, the other seven loci have not been studied directly in virulence models. We also used recombinase-based *in vivo* expression technology (RIVET) to identify promoters that are upregulated in *E. faecalis* OG1RF during *in vitro* biofilm growth (25). No common genes were found between the transposon and biofilm RIVET screens, but the screens were complementary in that there were four genomic regions with two adjacent genes where one gene was identified in the RIVET screen and the other gene was identified in the transposon screen. Two genes with transposon insertions encode transcriptional regulators, suggesting the possibility of regulatory interactions between these and the adjacent genes that were identified in the RIVET screen (25).

The ability to form biofilms is common among *E. faecalis* isolates of clinical origin (26, 27), but a broad analysis to identify the genetic loci on the *E. faecalis* chromosome that are responsible for biofilm-associated infection has not been undertaken. We postulated that screening the potential biofilm determinants identified in our previous genetic screens for roles in virulence in an animal model of biofilm infection would lead to the discovery of new biofilm-associated virulence factors. Therefore, the purpose of this study was to identify biofilm formation genes in *E. faecalis* OG1RF that contribute to the pathogenesis of endocarditis. To that end, we tested whether five of the biofilm-defective transposon insertion mutants (20) were attenuated in a rabbit model of endocarditis. In addition, we sought to test whether the complementary outcome of the combined results of our previous transposon and RIVET screens predicted regulatory interactions among biofilm-associated genes (25). To do this, we characterized the biofilm formation and endocarditis virulence phenotypes of two strains with in-frame deletions of genes identified in our RIVET screen that are adjacent to the two biofilm-associated ArgR family transcriptional regulators identified in the transposon screen. We show here that the *E. faecalis* ortholog of the ArgR family transcription factor AhrC is an important early biofilm gene product that is necessary for endocarditis virulence. Our data further reveal that AhrC and Eep, the endocarditis virulence factor we recently identified (13), are also important for virulence in an experimental biofilm infection model of catheter-associated UTI. Overall, the data presented in this study demonstrate that novel

virulence factors with important *in vivo* functions can be identified from *in vitro* functional screens.

MATERIALS AND METHODS

Bacterial strains, growth conditions, and chemicals. *E. faecalis* strains used in this study are listed in Table 1. *E. faecalis* was routinely cultivated in brain heart infusion broth (BHI) (BD Bacto; Becton, Dickinson and Company, Sparks, MD) or on BHI agar under static conditions at 37°C in ambient air. Cultures for endocarditis experiments were grown in trypsinized beef heart dialysate (BH) medium (28) under static conditions at 37°C with 7% CO_2. Tryptic soy broth without added dextrose (TSB$_{-dex}$; Becton, Dickinson, and Company) was used for biofilm assays. M9-YE glucose medium (29) was used to grow cells for Western blot experiments. *Escherichia coli* strains DH5α and EC1000 were used for plasmid construction and propagation and were grown in LB and BHI, respectively. Antibiotics were added as necessary to select and maintain plasmids.

Nisin, erythromycin, carbenicillin, and kanamycin were purchased from Sigma-Aldrich (St. Louis, MO). Stock solutions of nisin at 25 µg/ml in water, erythromycin at 50 mg/ml in methanol, carbenicillin at 50 mg/ml in water, and kanamycin at 100 mg/ml in water were prepared and stored at −20°C. All restriction enzymes were purchased from New England BioLabs (Ipswich, MA). *PfuUltra* II fusion DNA polymerase (Agilent Technologies, Santa Clara, CA) or *Taq* DNA polymerase with Thermopol buffer (New England BioLabs) was used in PCRs for strain and plasmid construction. Oligonucleotides were synthesized by Invitrogen (Carlsbad, CA) or Integrated DNA Technologies (Coralville, IA) and are listed in Table 1.

Strain construction. The in-frame markerless deletion of the *recN* (EF0984) locus was previously described in an OG1RF(pCF10) strain (25). The same constructs and procedures were used in this study to generate a pCF10-free version of OG1RF Δ*recN*. OG1RF Δ*opuBC* (EF0675) was constructed using the previously described allelic exchange method (30). The deletion construct used for allelic exchange was generated with overlap-extension PCR by first amplifying two ~1-kb fragments from OG1RF genomic DNA with primer pairs 0674 Xba F/Delta 0675 R and Delta 0675 F/0677 R SphI. The two products were annealed together, and second step amplification was performed with primers 0674 XbaI F and 0677 R SphI. The resulting product was digested with enzymes XbaI and SphI, ligated into pCJK47 (30) predigested with the same enzymes, and propagated in *E. coli* EC1000 grown on BHI with 100 µg/ml erythromycin. Deletion of either locus had no effect on growth (data not shown).

The OG1RF Ω*ahrC*-p$_{23}$*ahrC*KI strain was generated by allelic exchange using pCJK141, a derivative of pCJK47 that facilitates integration of constructs into the OG1RF chromosome between the convergently transcribed genes EF1117 and EF1116 (31). The 196-nucleotide intragenic region between EF1117 and EF1116 contains a stem-loop transcriptional terminator (32), which has been duplicated in the cloning site of pCJK141 so that sequences integrated into the chromosome are flanked by terminators to prevent transcriptional read-through in either direction. To generate the knock-in p$_{23}$ construct, the *ahrC* gene—including its native ribosome binding site (RBS)—was PCR amplified from OG1RF genomic DNA using primer pair 0983 RBS BamHI F/0983 st cod NcoI R, and ligated into pCJK141 at the BamHI and NcoI restriction sites in the multiple cloning site of the vector. A PCR product containing the p$_{23}$ promoter, originally from *Lactococcus* sp. (33), was generated with primer pair NotI P23/BamHI P23 and was introduced upstream of *ahrC* in pCJK141 at the NotI and BamHI restriction sites.

Rabbit model of experimental endocarditis. Endocarditis infections were carried out as previously described (34). Briefly, one to three colonies of each strain were inoculated into BH medium and grown overnight. Cultures of OG1RF Ω*ahrC*+*ahrC* also contained 10 µg/ml erythromycin and 25 ng/ml nisin. Cells were pelleted and resuspended to an optical density at 600 nm (OD$_{600}$) of 1.0 in potassium phosphate-buffered saline (KPBS), corresponding to ~2 × 10^9 to 4 × 10^9 CFU/ml. Following sur-

TABLE 1 *Enterococcus faecalis* strains and oligonucleotides used in this study

Strain or oligonucleotide	Strain description or oligonucleotide sequence	Source or reference
Strains		
OG1RF	Wild-type strain	60
OG1RF $\Delta opuBC$	Markerless in-frame deletion of locus EF0675	This study
OG1RF $\Delta recN$	Markerless in-frame deletion of locus EF0984, remade in a pCF10-free background in this study	25; this study
OG1RF Δeep	Markerless in-frame deletion of locus EF2380, also called JRC106	30
OG1RF $\Omega argR$	Transposon mutant 17M8, disruption in EF0676	20
OG1RF $\Omega atlA$	Transposon mutant 25G5, disruption in EF0799	20
OG1RF $\Omega ahrC$	Transposon mutant 20K19, disruption in EF0983	20
OG1RF $\Omega sepF$	Transposon mutant 30B8, disruption in EF0999	20
OG1RF $\Omega pyrC$	Transposon mutant 39F15, disruption in EF1718	20
OG1RF $\Omega ahrC+ahrC$	Transposon mutant 20K19 ($\Omega ahrC$) with complementation plasmid pCJK124, a pMSP-3535-based vector with a nisin-inducible promoter driving expression of *ahrC*	20
OG1RF $\Omega ahrC$-p$_{23}ahrC$KI	Transposon mutant 20K19 ($\Omega ahrC$) with *ahrC* ORF (EF0983) and native RBS fused downstream of the p$_{23}$ promoter and integrated into the chromosome between EF1117 and EF1116	This study
Oligonucleotides		
0674 XbaI F	CTAGTATCTAGAGACAGGTGAAGTGGCTCTCAATGAAC	This study
Delta 0675 R	GTAAAAAATACTTATTTAAGAAGTGCTTGCATCTACTATCCCTC	This study
Delta 0675 F	TAGTAGATGCAAGCACTTCTTAAATAAGTATTTTTTACTG	This study
0677 R SphI	CTAGTAGCATGCGCGTCGTAGCTAAACCAACGTC	This study
0983F-RT	GAAAAGGGCGTAGCTGTAACAC	This study
0983 RBS BamHI F	CTGTAGGGATCCGAGTAAACTGAAAAGGAGAGCG	This study
0983 st NcoI R	CTGTATCCATGGCATTCTTTATAGATAGCTTAACAGC	This study
BamHI P23	ATAGTAATAAGCGGCCGCAAAGCCCTGACAACGC	This study
NotI P23	GAGTGGATCCTTTTTAATTTAATTCTAAGACTATTTTATC	This study
EF0983-F	ATGAGAAAGCAAGATAGACACC	This study
EF0983-R	TTATAGATAGCTTAACAGCTC	This study
gelE forward	CTTTTTGGGATGGAAAAGCA	39
gelE reverse	CCGGCAGTATGTTCCGTTAC	39
gelE ORF-F	TCATTCATTGACCAGAACAGA	This study
gelE ORF-R	ATGAAGGGAAATAAAATTTTATAC	This study

gery to mechanically damage the aortic valve (34), 2 ml was administered intravenously via the marginal ear vein to initiate infection. Rabbits were euthanized 4 days after infection, and the hearts were removed and dissected to expose the aortic valve. Vegetations and valve leaflets were harvested, weighed, homogenized in 1 ml of Todd-Hewitt broth (THB) or KPBS, serially diluted, and plated on BHI agar to quantify bacteria. Homogenates from animals infected with OG1RF $\Omega ahrC+ahrC$ were also plated on BHI agar containing 10 µg/ml erythromycin to determine the percentage of cells that retained the complementation vector for the duration of the infection.

Endocarditis results were analyzed for statistical significance with one-way analysis of variance (ANOVA), followed by Bonferroni's multiple comparison tests in GraphPad Prism (version 5.04; GraphPad Software, Inc., La Jolla, CA).

Murine model of CAUTI. OG1RF, OG1RF $\Omega ahrC$, and OG1RF Δeep were tested in a mouse model of catheter-associated urinary tract infection (CAUTI) as previously described (12). Briefly, $\sim 1 \times 10^7$ bacteria were inoculated into C57BL/6Ncr female mice that had silicone catheter pieces implanted in their bladders. Eight to 10 mice were infected per strain. Animals were euthanized 24 h postinfection by cervical dislocation, and then catheter implants, bladders, and kidney pairs were harvested. Bacterial counts from implants, bladders, and kidney pairs were obtained as previously described (12). The limits of detection (LOD) were 20 CFU per implant and 40 CFU per bladder or pair of kidneys. Implants or organs with bacterial counts below the LOD were assigned the LOD value for statistical calculations. The experiment was repeated once, and the results were pooled. Only mice from which implants were recovered at the time of sacrifice were included in the final analysis. The Mann-Whitney U test in GraphPad Prism was used to assess statistical significance.

Microtiter plate biofilm assay. Microtiter plate biofilm assays were based on a previously described protocol, with minor changes (35). Briefly, three colonies per strain were inoculated into 2-ml BHI cultures and grown overnight. Cultures were diluted 1:100 in TSB$_{-dex}$, and 100 µl of each diluted strain was pipetted into 8 wells of a 96-well plate (Costar 3595; Corning, Inc., Corning, NY). All cultures of OG1RF $\Omega ahrC+ahrC$ also contained 10 µg/ml erythromycin and 25 ng/ml nisin. Wells with sterile medium were used as blanks. Plates were statically incubated at 37°C for 6 or 24 h in a humid container. Culture turbidity was assessed following incubation by reading the optical density at 600 nm (OD$_{600}$) on a Modulus microplate multimode reader (Turner Biosystems, Sunnyvale, CA). The medium was removed, wells were washed three times with 100 µl water, and plates were dried in an inverted position for at least 4 h. Wells were stained with 100 µl of 0.1% safranin for 20 min, and then the stain was removed and wells were washed five times with water and dried for at least 4 h. The safranin stain was quantified by reading the optical density of dried wells at 450 nm. Three to six biological replicates were performed for each strain. The OD$_{450}$ values for all biological replicates were averaged together and reported as percent biofilm formation relative to OG1RF, which was set to 100%.

Biofilm microscopy. *E. faecalis* OG1RF and $\Omega ahrC$ biofilms were inoculated at a 1:50 dilution from overnight cultures and grown on Aclar fluoropolymer coupons for 6 h and washed for imaging as previously described (13). Coupons were stained with an Alexa Fluor 594-wheat germ agglutinin conjugate (Invitrogen) and fixed in 2% methanol-free formaldehyde with 6% sucrose added to avoid hypoosmolality. Coupons were rinsed in PBS and mounted in Vectashield Hardset (Vector Laboratories, Burlingame, CA) with coverslip spacers to avoid mechanical compression of the biofilm. Biofilm imaging was done using a 20× 0.75 NA

objective using an electron-multiplying charge-coupled device (EMCCD) camera (Cascade 1024; Photometrics, Tucson, AZ). Image stacks were collected at 0.5-μm intervals in wide-field immunofluorescence mode and deconvolved with the Huygens software package (SVI, Hilversum, The Netherlands). The COMSTAT2 analysis package (36, 37) was used to provide quantification of the *ahrC* mutant biomass defect; reported results are from four independent stacks taken on each of 10 biological replicates for both the mutant and wild-type strains. Maximum-intensity projections of the mean image stacks and surface renderings of representative stacks were also generated (Huygens software package).

Gene expression experiments. For growth curves, overnight cultures of OG1RF were diluted 1:1,000 into 100 ml of fresh BHI and grown statically at 37°C. Aliquots were collected at 0, 3.16, 4.1, 5.3, 6.5, and 8.25 h after inoculation for quantitation by serial dilution and plating. Cells for RNA extraction were harvested at 3.16 h and all following time points by measuring the optical density of the culture at 600 nm and then calculating the volume required to reach the equivalent of 0.6 ml at an OD_{600} of 1.0. The calculated volume of cells was pelleted, resuspended in KPBS, and treated with RNAprotect bacterial reagent (Qiagen, Inc., Valencia, CA) according to the manufacturer's protocol. Three biological replicates were performed. For biofilms, overnight cultures of OG1RF were diluted 1:100 into TSB$_{-dex}$, and then 3-ml aliquots were placed into 6-well dishes (Costar 3516; Corning, Inc.) and shaken at ~125 rpm for 6 or 22 h at 37°C. After incubation, planktonic cells were pooled and aliquots were collected for cell counts or treated with RNAprotect bacterial reagent for subsequent RNA extraction. Biofilms were gently washed twice with 1 ml KPBS and then manually removed with a cell scraper into 1 ml KPBS, which was transferred to each successive well in order to pool all biofilms grown in a single dish. Six wells were pooled for 6-h biofilms, and five wells were pooled for 22-h biofilms. Due to loss of volume during transfer, the final volume of pooled cells was adjusted to 1 ml with KPBS. One hundred microliters was kept for cell counts prior to adding the remainder to RNAprotect bacterial reagent. Planktonic cells were collected from five biological replicates. Biofilm cells were collected from six biological replicates.

All cell pellets treated with RNAprotect bacterial reagent were kept frozen until RNA extraction, which was performed as previously described (13). One microgram of each RNA was treated with Turbo DNA-free (Ambion, Austin, TX) according to the "Rigorous protocol" as directed by the manufacturer. cDNA was synthesized from 9 μl of DNase-treated RNA with random hexamer primers using the Superscript III first-strand synthesis system for reverse transcription (RT)-PCR (Invitrogen). cDNA was diluted 5-fold for growth curve time points and 2-fold for 6-h planktonic and biofilm samples and was used undiluted for 22-h planktonic and biofilm samples. One microliter of diluted or undiluted cDNA was used per 25-μl reaction mixture with iQ SYBR green Supermix (Bio-Rad Laboratories, Inc., Hercules, CA) and 10 μM each primer. Reaction mixtures containing ~12 ng of DNase-treated RNA were prepared to confirm successful removal of contaminating DNA. Quantitative PCR (qPCR) was carried out on an iQ5 iCycler real-time detection system (Bio-Rad). Each reaction was performed in triplicate, and threshold cycle values were averaged.

Primers used in qPCR and for generating copy number standards are listed in Table 1. Absolute quantification of transcript copy number was calculated by interpolating threshold cycle values against standard curves, as described previously for *Staphylococcus aureus* (38). To prepare the standard curves, the *gelE* and *ahrC* genes were PCR amplified in standard PCRs using *Taq* polymerase with primer pairs gelE ORF-F/gelE ORF-R and EF0983-F/EF0983-R, respectively. PCR products were ligated into pGEM-T Easy (Promega Corp., Madison, WI) and propagated in *E. coli* DH5α on LB containing 50 μg/ml carbenicillin. Ten-fold dilutions of plasmid DNA prepared with the QIAprep spin miniprep kit (Qiagen, Inc.) were used as the templates in qPCR standard curve amplification reactions. For cDNAs that were diluted prior to qPCR, copy numbers were multiplied by the dilution factor to calculate the copy number per μl of

undiluted cDNA. Since unequal numbers of cells were harvested from planktonic/biofilm experiments, the relative gene expression was calculated by dividing the copy number per μl of cDNA by the corresponding CFU/ml count.

Recombinant His-tagged AhrC purification, antisera, and Western blots. The *ahrC* gene, including its native ribosome binding site, was PCR amplified and ligated into the pET28b(+) expression vector (EMD Millipore Corporation, Billerica, MA). The resulting plasmid was used to express and purify the recombinant His-tagged protein in *E. coli* BL21 cells under the growth conditions used for the purification of other *E. faecalis* proteins (39). Briefly, an overnight culture of BL21 carrying the expression vector was diluted 1:100 into LB containing 50 μg/ml kanamycin and shaken at 30°C until cells reached an OD_{600} of 0.7. IPTG (isopropyl-β-D-thiogalactopyranoside) was added to a final concentration of 1 mM, and the cells were incubated for 4 h. Protein was purified as previously described (40) and eluted in buffer containing 200 mM imidazole, 30 mM Tris-HCl (pH 7.5), 0.5 M NaCl, and 10% glycerol. The protein was dialyzed overnight at 4°C in elution buffer lacking imidazole.

Polyclonal antisera against recombinant AhrC protein was generated in a New Zealand White rabbit using standard procedures. The rabbit was immunized three times at 2-week intervals with 10 μg purified recombinant His-tagged AhrC per injection.

Cultures of M9-YE inoculated with three colonies of OG1RF, OG1RF Ω*ahrC*, or OG1RF Ω*ahrC*-p$_{23}$*ahrC*KI were grown overnight at 37°C and then diluted 1:10 or 1:100 and grown for 2 more hours. Whole-cell lysates were prepared from aliquots of cells harvested from overnight (stationary) or 2-h (exponential) cultures normalized to an OD_{600} of 1. Pelleted bacteria were resuspended in TES buffer (10 mM Tris [pH 8.0], 1 mM EDTA [pH 8.0], 25% sucrose) containing 15 mg/ml lysozyme and incubated at 37°C for 15 min. Cell lysis supernatants were subjected to SDS-polyacrylamide gel electrophoresis using standard protocols. Separated proteins were transferred to nitrocellulose membranes, which were blocked overnight with 10% milk in KPBS–0.1% Tween 20 at 4°C. Membranes were probed at room temperature for 1 to 2 h with a 1:4,000 dilution of the polyclonal anti-AhrC antiserum in blocking solution, washed with KPBS–0.1% Tween 20, and secondarily probed with a 1:5,000 dilution of horseradish peroxidase (HRP)-goat antirabbit IgG (H+L) antibody (Zymed; Invitrogen) in blocking solution for 1 to 2.5 h. Washed membranes were treated with the SuperSignal West Pico chemiluminescent substrate kit (Thermo Scientific, Rockford, IL) according to the manufacturer's instructions and exposed to film or a chemiluminescent imaging documentation system to detect signals. Two to three biological replicates were performed for each strain. Band densitometry was performed with ImageJ software (version 1.46r).

RESULTS

Biofilm-associated mutants tested in this study. To test the hypothesis that enterococcal biofilm determinants are virulence factors in endocarditis, we chose seven loci (Table 1) in the chromosome of *E. faecalis* OG1RF that were associated with biofilm formation in our previous studies (20, 25). The following five loci were disrupted with transposon insertions: EF0676, EF0799, EF0983, EF0999, and EF1718. The other two loci, EF0675 and EF0984, were removed from the chromosome as in-frame deletions generated by allelic exchange. Aside from EF0799, the functions of the selected loci in enterococcal biofilm formation or virulence have not been characterized. EF0799, which encodes the autolysin AtlA (also called Atn), has biofilm-associated functions (23, 41) but does not contribute to virulence in peritonitis or UTI models (12, 24). The phenotype of an *atlA*-deficient strain in endocarditis has not been reported previously.

EF0984 and EF1718 are annotated in the *E. faecalis* V583 genome sequence available through the J. Craig Venter Institute (JCVI) as encoding the highly conserved orthologs of DNA repair

TABLE 2 Gene assignments based on amino acid homology for previously unassigned *E. faecalis* loci tested in this study

Locus	Gene name	Gene function	BLASTP % identity/similarity, organism	NCBI accession no. for sequence used in BLASTP alignment
EF0675	*opuBC*	Glycine betaine/choline-binding protein of an ABC-type transporter	62/80, *Streptococcus mutans*	NP_721486.1
EF0676	*argR*	Transcriptional regulator	34/60, *Lactococcus lactis* subsp. *cremoris*	AAR99639.1
EF0983	*ahrC*	Transcriptional regulator	36/56, *Lactococcus lactis* subsp. *cremoris*	AAR99642.1
EF0999	*sepF*	Cell division protein	52/75,[a] *Bacillus subtilis*	NP_389422.2

[a] Homology based on amino acids 123 to 207 of the EF0999 protein sequence.

protein RecN (*recN* gene) and dihydroorotase (*pyrC* gene), respectively. Gene assignments for the remaining loci were made based on amino acid sequence homologies (Table 2). EF0675 encodes a glycine betaine/choline-binding protein of an ABC-type transporter that is highly similar to the *opuBC* gene annotated in *Streptococcus mutans*; we have designated EF0675 as the *opuBC* ortholog of *E. faecalis*. EF0999 is annotated as a conserved hypothetical protein in strain V583 and a hypothetical protein in the *E. faecalis* OG1RF genome sequence (GenBank accession no. CP002621.1) housed at the National Center for Biotechnology Information (NCBI), but contains a conserved region of homology in its C-terminal half that is found in the *sepF* loci of other Gram-positive microbes. Thus, we have designated EF0999 as the *sepF* ortholog (also called *ylmF*) in *E. faecalis* OG1RF. SepF/YlmF has been shown to associate with FtsZ during cell division in *Bacillus subtilis* (42, 43).

The loci disrupted in transposon insertion mutants ΩEF0676 and ΩEF0983 encode related ArgR/AhrC family transcriptional regulators. As indicated in Table 2, the amino acid sequence of EF0676 is most similar to ArgR of *Lactococcus lactis* subsp. *cremoris* MG1363, while that of EF0983 is most similar to AhrC of the same *Lactococcus* strain (44). In addition, EF0983 is adjacent to the open reading frame (ORF) encoding *recN*, which is a conserved genomic organization found in other Gram-positive bacteria (45). EF0676 is annotated as the arginine repressor *argR* in the *E. faecalis* V583 genome sequence at JCVI, but was generically assigned the gene symbol *argR2* (locus OG1RF_10413) in the OG1RF genome at NCBI. Likewise, EF0983 has been assigned the gene symbol *argR3* (locus OG1RF_10717) in the NCBI OG1RF genome annotation. There are two additional ArgR-like transcription factors in the OG1RF genome, encoded by the adjacent, but divergent, loci EF0102 and EF0103. These genes lie immediately upstream of the arginine catabolism genes and were referred to as *argR2* and *argR1*, respectively, in an older study (46). Due to the high sequence homology and conserved genome organization with species in which these genes have been characterized, we believe the most accurate gene names for EF0676 and EF0983 are *argR* and *ahrC*, respectively, and refer to them as such herein.

Characterization of the role of biofilm determinants in early biofilm biomass accumulation. The transposon mutants chosen for this study were previously shown to be deficient for biofilm formation using a microtiter plate biofilm assay that primarily evaluates initial attachment and early biomass accumulation (20). The time points at which the transposon strains' defects affect biofilm formation prior to the 24-h assay endpoint are not known. In addition, the phenotypes of the two in-frame deletion mutants (Table 1) in the microtiter plate biofilm assay are unknown. This led us to test the seven strains for biofilm formation at 6 and 24 h.

Defects in biofilm biomass accumulation by the transposon mutants at 24 h (Fig. 1) were consistent with our previous results (20), except that the Ω*sepF* strain produced more biofilm than in our previous report (20). At 6 h, the biofilm biomass value for Ω*sepF* was only slightly lower than the same value for OG1RF (Fig. 1). The biofilm biomasses of the other four transposon mutants fell below the line at 75% biofilm biomass relative to OG1RF, which was the level we previously used to define reduced biofilm formation (20). The early biofilm defect was most pronounced for the Ω*argR* and Ω*ahrC* transcription factor mutants, suggesting these strains are deficient in initial attachment in this experimental system. The early biofilm defect was fully restored (Fig. 1) by expression of the *ahrC* ORF from both an inducible promoter on a plasmid, as was previously shown for 24-h biofilms (20), and the constitutive lactococcal p_{23} promoter integrated into the chromosome at an ectopic site (described further below).
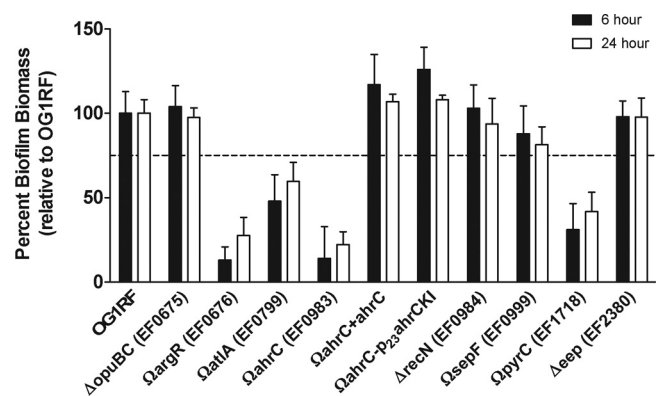
The Δ*opuBC* and Δ*recN* strains both produced biofilms at

FIG 1 Characterization of the role of biofilm determinants in biofilm biomass accumulation at 6 and 24 h. Biofilm biomass accumulation after 6 (black bars) and 24 (white bars) h in a microtiter plate biofilm assay was measured for *E. faecalis* wild-type strain OG1RF and seven strains with either *mariner* transposon insertions (designated by Ω in the strain name) or in-frame markerless deletions (designated by Δ in the strain name) in previously identified biofilm determinant genes (20, 25). The Ω*ahrC*+*ahrC* strain carries plasmid pCJK124 (20), a pMSP3535-based vector with the *ahrC* open reading frame cloned downstream of a nisin-inducible promoter. The Ω*ahrC*+p_{23}*ahrC*KI strain constitutively expresses the *ahrC* open reading frame from the p_{23} promoter at an ectopic chromosomal location, as described in the text. The mean absorbance for n = 2 to 6 biological replicates per strain is graphed as percent biofilm biomass relative to OG1RF, which was set to 100%. Error bars represent standard deviations (SD). The mean absorbances ± SD for OG1RF were 0.092 ± 0.012 for 6 h and 0.126 ± 0.010 for 24 h (n = 6 for both time points). The dotted line at 75% represents the level used to define reduced biofilm accumulation in our previous genetic screen for biofilm-defective transposon insertion mutants (20).
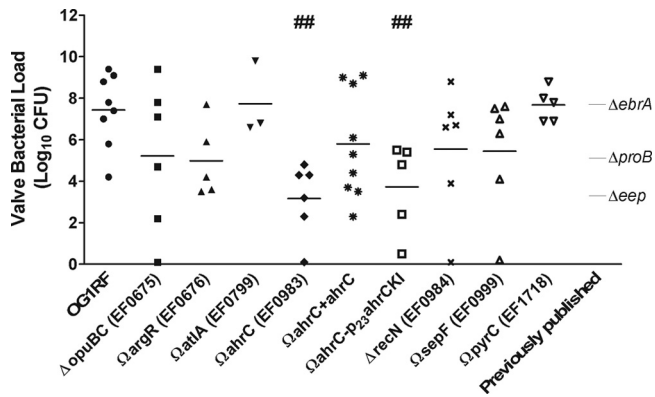
FIG 2 Role of biofilm determinants in experimental endocarditis virulence. Aortic valve leaflets and vegetations from rabbits in which *E. faecalis* endocarditis had been induced were harvested, homogenized, and plated to enumerate bacteria at 4 days postinoculation. Each symbol represents the $\log_{10}$ valve bacterial load for an individual animal. Thick horizontal bars show the arithmetic mean of the $\log_{10}$-transformed values. For comparison, the arithmetic mean $\log_{10}$ valve bacterial loads for the $\Delta ebrA$, $\Delta proB$, and Δeep strains tested in the same experimental endocarditis model in a previous study (13) are shown at the far right (thin horizontal bars). OG1RF, $n = 8$; $\Delta opuBC$, $n = 6$; $\Omega argR$, $n = 5$; $\Omega atlA$, $n = 3$; $\Omega ahrC$, $n = 6$; $\Omega ahrC + ahrC$, $n = 9$; $\Omega ahrC$-$p_{23}ahrC$KI, $n = 5$; $\Delta recN$, $n = 6$; $\Omega sepF$, $n = 6$; $\Omega pyrC$, $n = 5$. ##, $P < 0.05$ by one-way ANOVA followed by Bonferroni's multiple comparison test.

near-wild-type levels at 24 h (data not shown). These results are consistent with the biofilm formation phenotypes of three other in-frame deletion strains, including Δeep, that were characterized subsequent to the corresponding genes being identified in our previous RIVET studies (13). At 6 h, biofilm formation for the $\Delta opuBC$ and $\Delta recN$ strains was equivalent to that of the wild type. The Δeep strain, which was included in Fig. 1 for comparison, also showed no early biofilm formation defects in the microtiter plate biofilm assay (13).

Role of biofilm determinants in endocarditis virulence. We next evaluated the seven strains for virulence in a rabbit model of endocarditis, as measured by the bacterial load recovered from harvested valve leaflets and vegetations that formed after 4 days of infection (Fig. 2). Initial infections using 3 to 5 animals per strain were carried out in order to determine whether any strains retained wild-type virulence levels. Those lacking discernible decreases in valve bacterial loads after initial testing were not used in additional infection experiments, and the data from the initial tests are shown in Fig. 2. Strains that showed reduced bacterial loads were tested in additional animals, as indicated in Fig. 2. The mean valve bacterial loads of the $\Omega atlA$ and $\Omega pyrC$ strains were slightly higher than that for OG1RF. The $\Delta opuBC$, $\Omega argR$, $\Delta recN$, and $\Omega sepF$ strains had mean valve bacterial loads that were 1 to 2 $\log_{10}$ CFU lower than that for OG1RF. These values were not found to be significantly different from those for OG1RF in a statistical analysis. The $\Omega ahrC$ mutant mean valve bacterial load was significantly reduced compared to that of OG1RF. Interestingly, three in-frame deletion mutants, the $\Delta ebrA$, $\Delta proB$, and Δeep strains, which we previously tested in the same model system (13), showed a similar spread of mean valve bacterial loads (indicated in Fig. 2). Valve bacterial loads for the $\Omega ahrC$ and Δeep strains were both reduced by more than 4 $\log_{10}$ CFU compared to OG1RF ($P < 0.05$). Of the 10 total strains with mutations in biofilm-associated genes evaluated between this study and our previ-

ous work, the $\Omega ahrC$ and Δeep strains both had altered *in vitro* biofilm formation phenotypes (Fig. 1) (13) and were the most highly attenuated in endocarditis. These results show that certain enterococcal biofilm-associated genes are also important for virulence in a biofilm-associated infection.

As we previously demonstrated with the Δeep mutant strain (13), expression of the *ahrC* ORF from an inducible promoter on a plasmid enhanced the $\Omega ahrC$ endocarditis virulence phenotype (Fig. 2). The mean valve bacterial load of the complementation strain was 1.6 $\log_{10}$ CFU lower than that of OG1RF. This may be due in part to the lack of inducing agent required for maximal continued expression of the ORF and the absence of antibiotic selection required for plasmid maintenance in the host environment. Indeed, the complementation plasmid was only retained in 2.6% ± 3.3% (mean ± standard deviation [SD]) of cells by the end of the 4-day infection. These data are consistent with a model in which the functional role of AhrC in endocarditis occurs primarily during the early stages of infection. In light of the instability of the complementation plasmid, we generated a derivative of the $\Omega ahrC$ strain in which the *ahrC* ORF was integrated in the chromosome in single copy and expressed under the control of the constitutive lactococcal p_{23} promoter (33). When this strain was tested in endocarditis (Fig. 2), we were surprised to find that the strain was as attenuated as $\Omega ahrC$. Based on these results, we suspect that temporal regulation of the wild-type *ahrC* locus is necessary for virulence. Comparative analysis of *ahrC* expression from the wild-type and p_{23} promoters is presented below.

Evaluation of biofilm-associated endocarditis virulence factors in an experimental model of CAUTI. To test if *ahrC* and *eep* are important for virulence in a nonendocarditis biofilm infection model, we tested the two mutant strains in a recently established mouse model of enterococcal CAUTI (12). Bacterial counts determined from the bladders, kidneys, and catheter implants of mice after 24 h of infection are shown in Fig. 3. OG1RF was recovered at ~10^6 CFU from implants and bladders and ~10^4 CFU from the kidneys. The CFU levels of the Δeep mutant recovered from bladders were similar to those of OG1RF, while the levels recovered from implant surfaces were more variable. The median Δeep CFU counts from homogenized kidneys were 1 log lower than the OG1RF kidney CFU counts, which was a statistically significant difference; no bacteria were recovered for three animals in this cohort. $\Omega ahrC$ CFU counts were reduced by statistically significant amounts in the bladder and kidneys and on the implants. $\Omega ahrC$ was particularly defective in colonizing the kidneys, as CFU counts were above the limit of detection in only 5 of 14 mice (36%). The outcome of the CAUTI experiments indicates that *ahrC*, and to a lesser extent, *eep*, are also important for urovirulence.

Microscopic characterization of early-time-point $\Omega ahrC$ biofilms. Since *ahrC* is an important contributor to the virulence of two biofilm-associated infections, we used immunofluorescence microscopy to study the mutant strain's biofilm defect in detail. The maximum intensity projections of mean image stacks obtained from biofilms of OG1RF and the $\Omega ahrC$ strain grown for 6 h, which are shown in Fig. 4, demonstrate a significant defect in $\Omega ahrC$ strain biomass (Fig. 4A) compared to that of a matched OG1RF sample (Fig. 4B). The mean biomass difference is approximately 4-fold via quantitative COMSTAT2 analysis (data not shown) ($P = 0.001$ by Student's *t* test). The $\Omega ahrC$ defect was even more visually pronounced when the microscopy data were viewed
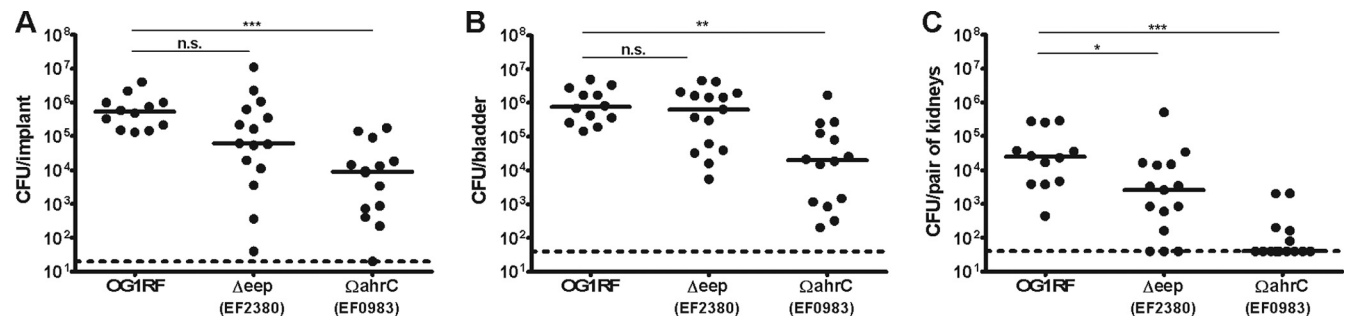
FIG 3 Enterococcal biofilm determinants important for endocarditis contribute to virulence in an experimental model of CAUTI. The graphs indicate the $\log_{10}$ CFU recovered from retrieved catheter implants (A), homogenized bladders (B), and homogenized kidneys (C) of mice implanted with silicone catheter pieces and subsequently infected with *E. faecalis* OG1RF ($n = 12$), the Δeep strain (EF2380; $n = 15$), or the $\Omega ahrC$ strain (EF0983; $n = 14$) for 24 h. Each symbol represents an individual animal, and only animals from which catheter implants were retrieved were included in the analysis. Horizontal bars represent the median, and the dashed lines indicate the limits of detection. *P* values were determined with the Mann-Whitney U test: n.s., not significant ($P > 0.05$); *, $P = 0.01$; **, $P = 0.0003$; and ***, $P < 0.0001$.

as surface projections (Fig. 4C and D): in addition to the overall biomass defect (Fig. 4C), 6-h $\Omega ahrC$ strain biofilms failed to produce mature microcolonies compared to OG1RF biofilms (Fig. 4D).

***ahrC* is maximally expressed during exponential phase.** We characterized expression of the *ahrC* locus during batch-phase growth and in biofilms to investigate further the idea that this gene is involved in early steps of biofilm formation and the pathogenesis of biofilm infections. In batch culture, the absolute copy number of *ahrC* transcripts was the highest between 3 and 5 h of growth, which correlated with the exponential growth phase (Fig. 5A). *ahrC* transcript copy numbers fell off sharply following entry into the stationary phase, dropping by 1 log between the 5.3- and 6.5-h time points. Notably, the expression profile of *ahrC* is distinct from that of *gelE* (Fig. 5A), which encodes the secreted protease gelatinase that is produced in postexponential phase as a result of activation of the quorum-sensing *fsr* gene cluster (47).

The relative levels of expression of *ahrC* and *gelE* were the same in biofilm cells [average ± SD, $(8.3 \pm 2.7) \times 10^8$ CFU/ml] and planktonic cells ($2.5 \times 10^8 \pm 8.6 \times 10^7$ CFU/ml) harvested from the same wells after 6 h of growth (Fig. 5B). Consistent with the data in Fig. 5A showing a decline in *ahrC* transcript levels over time, *ahrC* transcripts could not be detected in either planktonic [$(6.8 \pm 4.5) \times 10^8$ CFU/ml] and biofilm [$(6.0 \pm 2.2) \times 10^8$ CFU/ml] cells after 22 h of growth. In contrast, *gelE* transcripts were detected in planktonic and biofilm cells at 22 h.

Using a polyclonal antiserum raised against recombinant histidine-tagged AhrC, a strong immunoreactive protein band of the expected size was detected in exponential- and stationary-phase OG1RF whole-cell lysates, but not in exponential- or stationary-phase $\Omega ahrC$ cell lysates (Fig. 5C). The amount of AhrC in stationary-phase OG1RF preparations was calculated by densitometry to be reduced approximately 25% relative to that in exponential-phase cells. AhrC was highly overexpressed in $\Omega ahrC$-p$_{23}$*ahrC*KI exponential- and stationary-phase cells compared to OG1RF cells (Fig. 5C), suggesting that the p$_{23}$ promoter is much stronger than the native *ahrC* promoter under the conditions we analyzed.

DISCUSSION

Initial and irreversible attachment of bacteria to surfaces, followed by biomass accumulation, are the imperative first steps in the pro-

gression of biofilm formation (48). In endocarditis, blood-borne bacteria attach to host-derived collagen, fibrin, platelets, and occasionally red or white blood cells, to form vegetations at sites of damaged cardiac endothelium. Similarly, in CAUTI, bacteria in the urogenital tract interact with host proteins that adhere to the surfaces of urinary catheters. *E. faecalis* has many well-studied surface adhesins that likely facilitate the initial binding phases of heart valve vegetation formation or urinary catheter colonization, but other genes must be involved to coordinate the additional processes, such as extracellular matrix formation, immune evasion, and cell-to-cell communication, that lead to biomass accumulation and the subsequent proliferation of an established biofilm *in vivo*. It has been reported that *E. faecalis* endocarditis isolates make more biofilm biomass than nonendocarditis isolates in *in vitro* assays (27), but no strong linkages have been found between biofilm formation and the presence of various virulence factors in endocarditis and other clinical isolates (26, 49). Conversely, it has remained largely undefined to this point whether enterococcal biofilm genetic determinants correlate with virulence functions.

A major goal of this study was to determine whether gene function in biofilm formation is predictive of a function in endocarditis virulence. Since bacterial attachment to damaged heart valves is a critical step in the onset of infection, the majority of the seven strains we tested had transposon insertions in genes that affected 24-h biofilm formation in an assay that evaluates attachment (20). Although all of the transposon insertion mutants exhibited reduced early biofilm formation relative to OG1RF (Fig. 1), only the strain with a transposon disruption in the *ahrC* gene, encoding a transcriptional regulator, was highly attenuated in the endocarditis model (Fig. 2). AhrC was recently reported to regulate virulence gene expression in the human pathogen *Streptococcus pneumoniae* (45), but it was not tested for a direct role in virulence. The data presented here represent the first description of AhrC serving as a virulence factor in any bacterial pathogen.

The two chromosomal in-frame deletion strains, which had deletions in RIVET-identified genes (25) that were adjacent to either of the ArgR family transcriptional regulators identified as biofilm determinants in the transposon screen (20), were not impaired in biofilm formation or endocarditis virulence (Fig. 1 and 2, respectively). These data do not support our hypothesis that the combined results of the transposon and RIVET screens
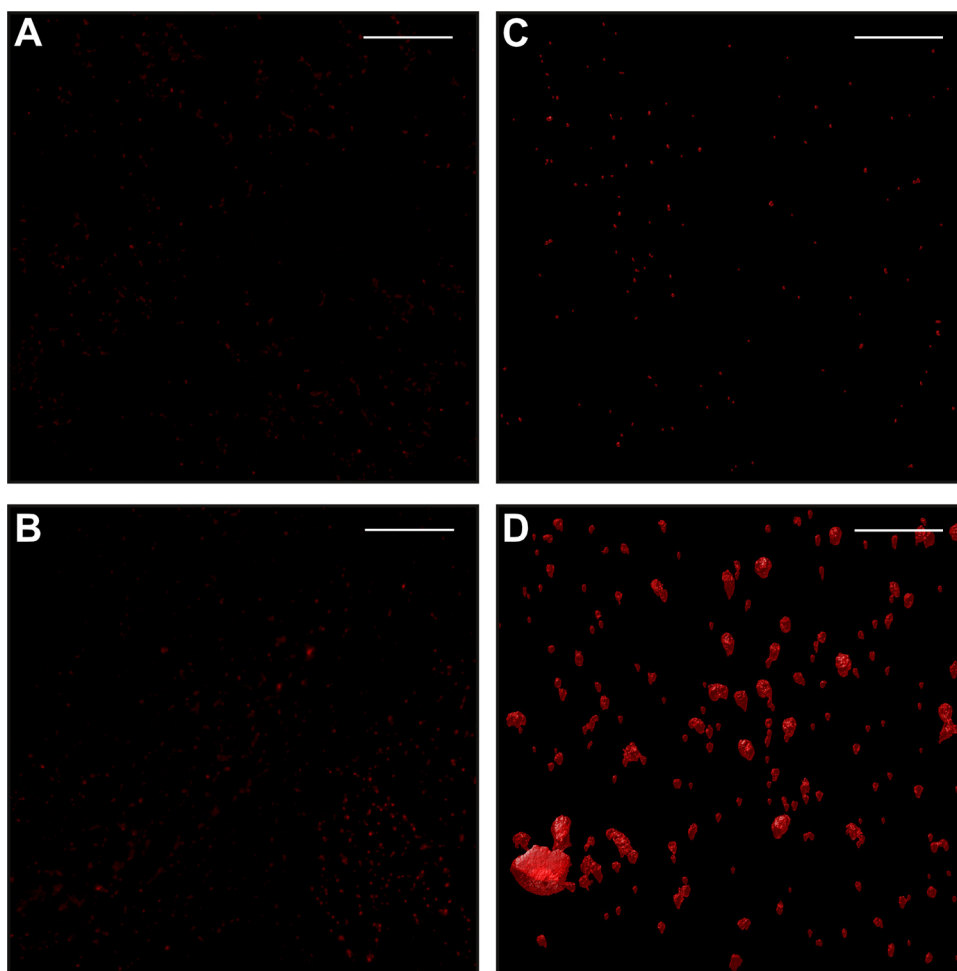
FIG 4 ΩahrC biofilms display a profound biomass defect in early biofilms. OG1RF and ΩahrC biofilms were grown on Aclar fluoropolymer coupons for 6 h. Biofilms were stained with an Alexa Fluor 594-wheat germ agglutinin conjugate and imaged as described in Materials and Methods. Simple maximum intensity projections of mean image stacks are shown for the ΩahrC strain (A) and a matched OG1RF sample (B). Biomass stack surface projections of the ΩahrC strain (C) and OG1RF (D) provide a modicum of depth information to the two-dimensional images. Scale bars, 20 μm.

reveal transcriptional regulatory networks. The genes deleted in these strains may have functions in infection or biofilm formation that are redundant with other genetic determinants, such that their phenotypes are masked in the assays used here. This precise type of effect has been reported with streptococcal adhesins (50, 51).

In combination with our previous work (13), we found that only 2 of the 10 biofilm-associated genes screened in the endocarditis model had significant roles in virulence. Five of the mutants tested between the two studies demonstrated an intermediate phenotype marked by valve bacterial loads that were nonsignificantly reduced by 1 to 2 $\log_{10}$ CFU relative to OG1RF (Fig. 2). The remaining three mutants had the same phenotype as OG1RF. It is noteworthy that the *atlA* disruption mutant displayed a wild-type virulence phenotype in endocarditis, which adds to previously published evidence that the major autolysin is not specifically relevant in virulence (12, 24), despite the availability of detailed knowledge about its mechanism in *in vitro* biofilm formation (Fig. 6) (20, 23, 41). From these results, we conclude that there is not a strong association between biofilm formation ability in static attachment assays and endocarditis virulence. Our group recently

reported that the processes of *E. faecalis* adherence and biofilm formation on *ex vivo* porcine cardiac valves proceed faster than on cellulose membranes (52). The interactions between bacteria and the host milieu that occur during *in vivo* biofilm formation are substantially more complex than the processes that result in biofilm formation in standard laboratory assays, such as the microtiter plate biofilm assay. The fact that the majority of the mutant strains tested in our combined studies exhibited either significant attenuation ($n = 2$) or had mean valve bacterial loads that were 1 to 2 $\log_{10}$ CFU lower than those of the wild type ($n = 5$) strongly indicates that the genetic basis of virulence in the endocarditis model is multifactorial. Some genes, such as *ahrC* and *eep*, are major contributors to the infection process, while a plethora of others serve more modest, and possibly functionally redundant, roles that act together to maximize the full virulence potential of *E. faecalis*. The absence of any mutants that were wholly unable to colonize and persist at the heart valve for the duration of a 4-day infection further supports the hypothesis that full endocarditis virulence results from the combined functions of multiple genetic determinants. Although it is impossible to predict how many genes contribute to endocarditis virulence, the *E. faecalis* strain
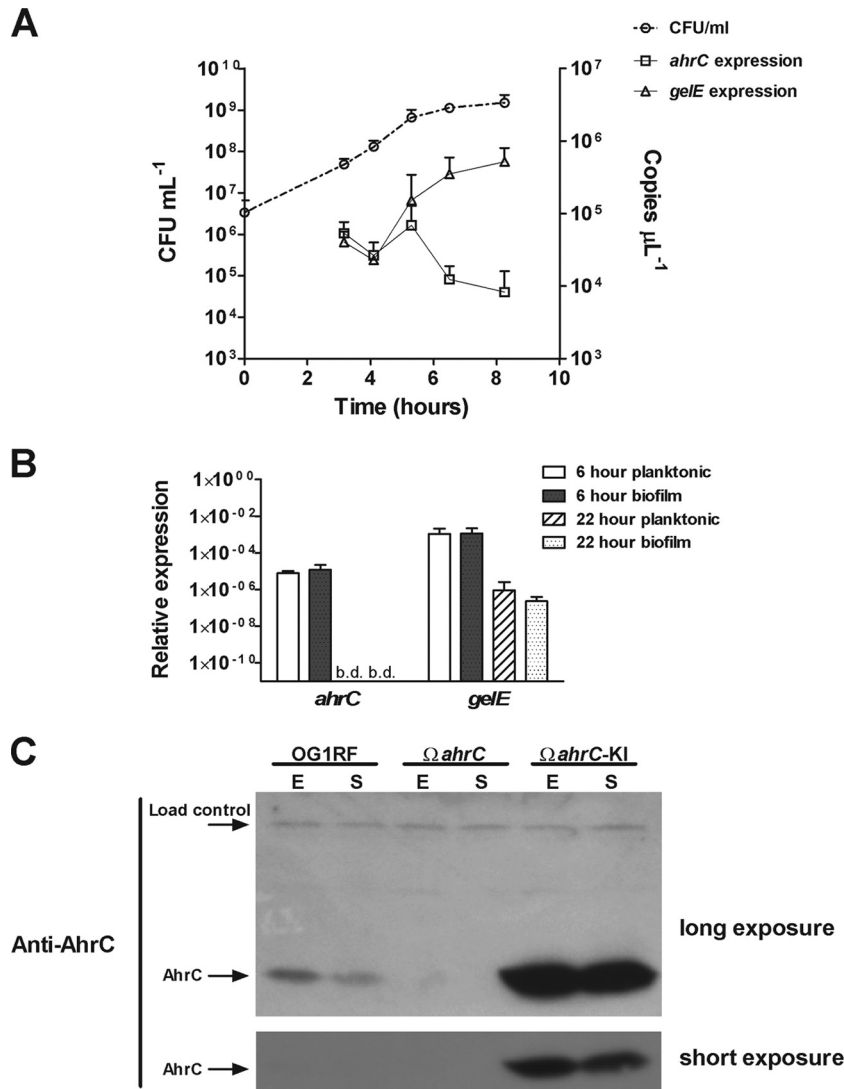
FIG 5 *E. faecalis* OG1RF *ahrC* expression at the RNA and protein levels. (A) Gene expression in batch culture. Aliquots of OG1RF cells growing in BHI were collected at the indicated time points and processed for quantitation by serial dilution and plating or for RNA extraction. Cell counts (circles connected by dashed line) correspond to the left *y* axis. cDNA copy numbers per μl for *ahrC* (squares) and *gelE* (triangles), included as a control for a gene known to be expressed in the stationary phase after cells reach an *fsr*-dependent quorum, correspond with values on the right *y* axis. Symbols are the mean of *n* = 3 biological replicates. Error bars represent standard deviations (SD). (B) Gene expression in biofilms. OG1RF planktonic and biofilm cells grown in plastic dishes in TSB$_{-dex}$ were harvested for quantitation and RNA extraction after growth for 6 or 22 h. Values are the means ± SD of *n* = 5 to 6 biological replicates collected on 2 separate days. Relative expression of *ahrC* and *gelE* was calculated by dividing the copies of detected transcript per μl of cDNA by the corresponding CFU/ml count from the harvested biofilm cells. b.d., below detectable limit of the qPCR assay. (C) Protein expression in early exponential and stationary phases. Whole-cell lysates of exponential (E)- or stationary (S)-phase cells were separated by SDS-PAGE, transferred to nitrocellulose, and probed with anti-AhrC polyclonal antisera. His-tagged AhrC is approximately 18 kDa. The upper band is a cross-reactive protein of unknown identity that was used as a loading control in densitometry measurements, which revealed that the relative amount of AhrC detected in stationary-phase OG1RF lysates was 25% less than the amount detected in exponential-phase lysates. Due to the strong overexpression of AhrC in the Ω*ahrC*-p$_{23}$*ahrC*KI strain (labeled "Ω*ahrC*-KI" on the figure for clarity), a shorter exposure of the same blot is shown in the bottom image. The top image was adjusted for brightness and contrast after densitometry in order to make the loading control bands visible for publication.

INY3000 has four mapped Tn*916* insertions in its genome and is avirulent in endocarditis (53–55).

Regardless of the low correlation between *in vitro* biofilm formation and virulence, this work resulted in the identification of two virulence factors that are important contributors in two animal models of biofilm-associated infection (Fig. 6). The *eep* and *ahrC* genes encode proteins that have dramatically different cellular functions. The *in vitro* biofilm phenotypes of the Δ*eep* and Ω*ahrC* strains display significantly different phenotypes: under *in*

vitro conditions, the Δ*eep* strain makes strong biofilms with an aberration in cell and matrix distribution (13, 56), while the data we report here indicate that the Ω*ahrC* mutant is defective in early attachment (Fig. 1) and biomass accumulation (Fig. 4). Despite this, disruption of either locus resulted in similar attenuated phenotypes in the rabbit endocarditis model (Fig. 2) (13). When assayed in a mouse model of CAUTI (Fig. 3), we found that Ω*ahrC* performed far worse in all variables tested than Δ*eep* did, although Δ*eep* was impaired in kidney colonization relative to OG1RF. A
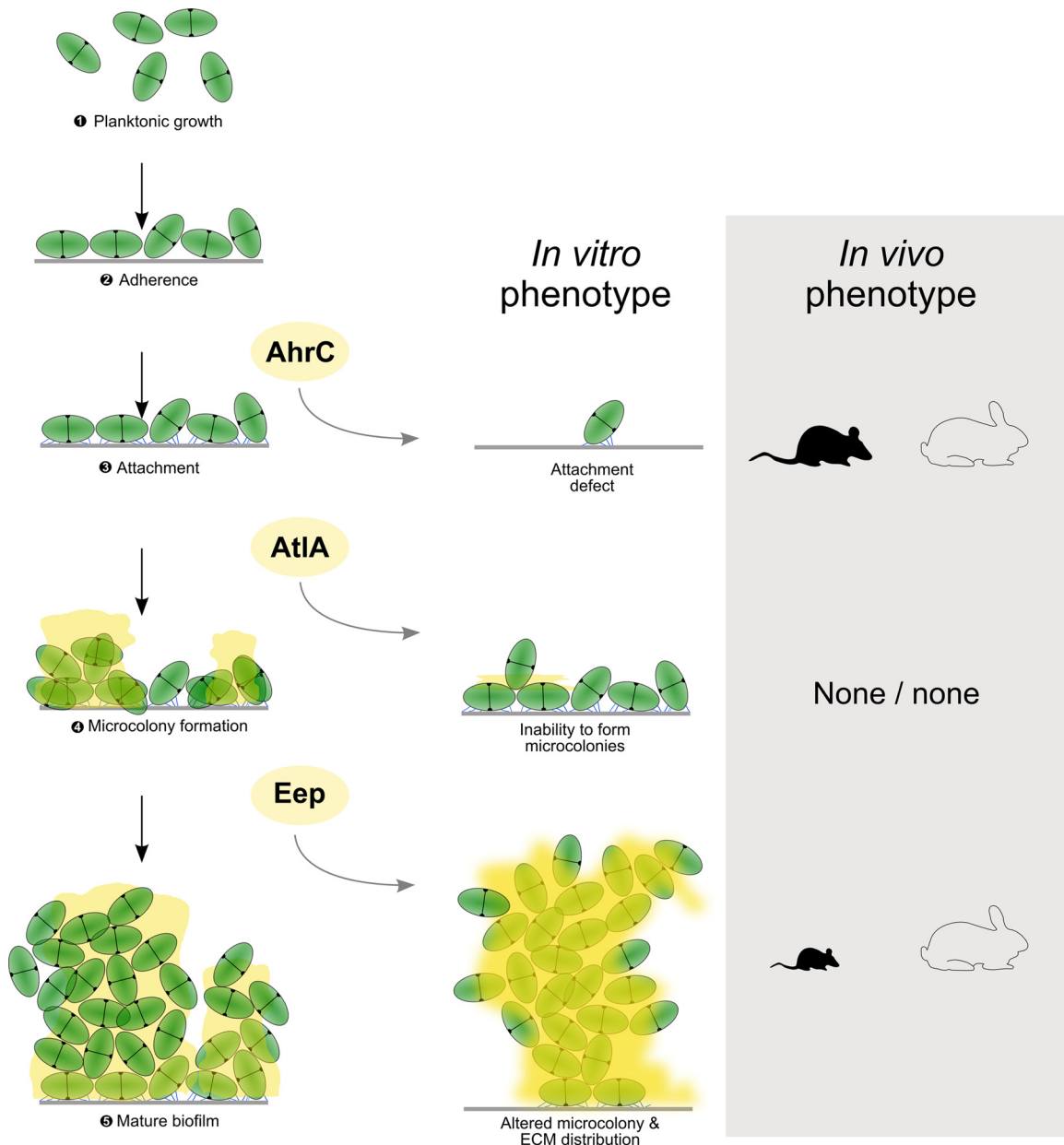
FIG 6 The biofilm genes *ahrC* and *eep*, but not *atlA*, are also virulence factors in biofilm-associated infections. The steps at which AhrC, AtlA, and Eep contribute to the process of biofilm formation are indicated (left). The center column illustrates the characterized biofilm phenotypes following disruption of the respective genes, while the right column summarizes the biofilm-associated infection models (mouse CAUTI or rabbit endocarditis) in which the respective genes contribute to virulence. The four other genes tested in this study were omitted from this figure because the biofilm phenotypes of strains lacking those genes have not been characterized in detail. Despite differences in protein function and roles in biofilm formation, AhrC and Eep are both virulence factors of biofilm-associated infections. The sizes of the mice in the image are scaled to reflect the severity of the attenuation phenotype measured for either *ahrC* or *eep*. Further experimentation is required to determine if the reason why the *ahrC* gene is a larger contributor than *eep* to CAUTI virulence is because of its role in the early biofilm stage of attachment. In contrast to AhrC and Eep, AtlA is important for microcolony formation during *in vitro* biofilm formation but makes no apparent contribution to *E. faecalis* virulence.

major difference between these two models is the presence of a foreign body in the CAUTI model, while the endocarditis model involves biofilm formation on a native host surface. The results from the infection models confirm that the pathogenesis of biofilm-associated infections differs from model to model. Given that only the Ω*ahrC* strain has an *in vitro* attachment defect, it may be that the mechanism of attachment employed during *in vitro* biofilm formation is also relevant to CAUTI pathogenesis, while

other mechanisms are at play in endocarditis. Overall, these experiments demonstrate that two major enterococcal endocarditis virulence factors may be more generally classified as virulence factors of biofilm-associated infections.

Since building a biofilm is a multistep process, the genes that are involved may act at one or more of the many steps along the progression of biofilm establishment and maturation (Fig. 6). This work demonstrates that disabling a strain such that it can no

longer proceed through these steps may or may not correlate with adverse effects in establishing a biofilm-related infection. For example, loss of AtlA impairs microcolony formation but does not reduce virulence in biofilm-mediated infections (Fig. 2 and 6) (12), while deletion of Eep imparts abnormal microcolony cell and matrix distribution and strongly suppresses vegetation formation during endocarditis and kidney colonization following CAUTI (Fig. 2, 3, and 6) (13). In the case of *ahrC*, Fig. 4 shows that Ω*ahrC* biofilms lagged behind OG1RF in the accumulation of stainable biomass after only 6 h of development, which is consistent with the early biofilm attachment defect in the microtiter plate assay shown in Fig. 1. Expression of *ahrC* was highest in planktonic cells during exponential growth of OG1RF (Fig. 5). Likewise, in the endocarditis complementation experiments using the nisin-inducible plasmid, *ahrC* expression was likely at its maximum in the inoculum since nisin was not present following injection of the bacteria into the rabbits. Thus, the data we present here collectively suggest that *ahrC* is important in the early stages of *E. faecalis* biofilm formation and endocarditis development (Fig. 6). This contrasts with expression of the gene encoding the extracellular protease GelE (Fig. 5), which is controlled by the quorum-sensing *fsr* locus (47). GelE functions at later stages in endocarditis by contributing to immune evasion and vegetation embolization (57).

It is unclear at this point what the specific role of AhrC is in the virulence of *E. faecalis* biofilm infections and whether this role is directly related to its role in *in vitro* biofilm formation. In other Gram-positive species, ArgR and AhrC regulate gene expression in response to arginine (45, 58). The *E. faecalis* AhrC and ArgR proteins may have related functions in biofilm formation since transposon insertions in either gene resulted in the smallest amount of attachment among the strains tested in early biofilms (Fig. 1). In preliminary experiments (data not shown), the addition of arginine to growth medium did not rescue the biofilm-defective phenotypes of either transposon strain, so it remains undetermined whether these genes function in response to arginine, as is seen in other species. Based on their disparate phenotypes in endocarditis virulence, it is clear these two transcription factors have different regulons within the context of the host environment. Experiments to characterize the *E. faecalis* AhrC regulon are needed, as they will provide insight into the regulatory pathways that function downstream of AhrC in *E. faecalis* endocarditis and *in vitro* biofilm formation.

The complementation strain that constitutively expresses *ahrC* from the chromosome restored the transposon insertion-mediated biofilm defect (Fig. 1), but unexpectedly failed to complement the endocarditis defect (Fig. 2). While it is possible that integration of the p$_{23}$*ahrC* construct into the chromosome between genes EF1117 and EF1116 disrupted a regulatory element or noncoding RNA that is specific for *in vivo* growth, the presence of an endogenous stem-loop transcriptional terminator upstream of the p$_{23}$*ahrC* integration site renders this scenario unlikely (32). We hypothesize that regulated expression of *ahrC* is critical for its function in virulence and that gross overproduction of AhrC in the chromosomal knock-in strain (Fig. 5) disrupted the ability of *E. faecalis* to establish infection at the heart valve surface. This would be the case if AhrC caused repression of genes that mediate later stages of endocarditis. The reason why overproduction of AhrC did not affect biofilm formation may be due to limitations of the microtiter plate biofilm assay being unable to segregate the

steps of biofilm formation beyond initial attachment and biomass generation. Alternatively, it is possible that high constitutive expression could result in promiscuous binding of the transcription factor to alternate promoters, resulting in incorrect expression of genes that affect infection-related functions irrelevant to *in vitro* biofilm formation. Further studies are needed to determine how *ahrC* expression is controlled. While our data (Fig. 5) confirm previously published results that the *ahrC* locus is not positively regulated by *fsr* (59), the possibility that transcription of *ahrC* is downregulated following *fsr* activation cannot be ruled out.

In conclusion, this study indicates that two of the biofilm determinants identified from transposon and RIVET genetic screens are virulence factors contributing to two distinct models of biofilm-mediated infection. The lack of a major role in endocarditis virulence for most of the biofilm genes tested here strongly suggests that the genetic requirements for *in vitro* biofilm formation and endocarditis do not significantly overlap. Both *eep* and *ahrC* are conserved in *Staphylococcus aureus*, thus making them attractive targets for the development of new vaccines or antimicrobial agents. Determination of the function of these enterococcal biofilm infection-associated virulence factors in biofilm formation and the establishment of disease is a source of ongoing study, as is testing the *S. aureus* homologs for functions in biofilm formation and infection. Overall, this research will improve our understanding of the mechanisms used by *E. faecalis* to colonize and form biofilms on surfaces inside a host.

REFERENCES

1. **Parsek MR, Singh PK.** 2003. Bacterial biofilms: an emerging link to disease pathogenesis. Annu. Rev. Microbiol. **57**:677–701.
2. **Hall-Stoodley L, Stoodley P.** 2009. Evolving concepts in biofilm infections. Cell. Microbiol. **11**:1034–1043.
3. **Hall-Stoodley L, Costerton JW, Stoodley P.** 2004. Bacterial biofilms: from the natural environment to infectious diseases. Nat. Rev. Microbiol. **2**:95–108.
4. **del Pozo JL, Patel R.** 2007. The challenge of treating biofilm-associated bacterial infections. Clin. Pharmacol. Ther. **82**:204–209.
5. **Coenye T, Nelis HJ.** 2010. In vitro and in vivo model systems to study microbial biofilm formation. J. Microbiol. Methods **83**:89–105.
6. **Kang J, Sickbert-Bennett EE, Brown VM, Weber DJ, Rutala WA.** 2011.

Relative frequency of health care-associated pathogens by infection site at a university hospital from 1980 to 2008. Am. J. Infect. Control **40**:416–420.

7. **Hidron AI, Edwards JR, Patel J, Horan TC, Sievert DM, Pollock DA, Fridkin SK.** 2008. NHSN annual update: antimicrobial-resistant pathogens associated with healthcare-associated infections: annual summary of data reported to the National Healthcare Safety Network at the Centers for Disease Control and Prevention, 2006–2007. Infect. Control Hosp. Epidemiol. **29**:996–1011.

8. **McDonald JR, Olaison L, Anderson DJ, Hoen B, Miro JM, Eykyn S, Abrutyn E, Fowler VG, Jr, Habib G, Selton-Suty C, Pappas PA, Cabell CH, Corey GR, Marco F, Sexton DJ.** 2005. Enterococcal endocarditis: 107 cases from the international collaboration on endocarditis merged database. Am. J. Med. **118**:759–766.

9. **Fernandez Guerrero ML, Goyenechea A, Verdejo C, Roblas RF, de Gorgolas M.** 2007. Enterococcal endocarditis on native and prosthetic valves: a review of clinical and prognostic factors with emphasis on hospital-acquired infections as a major determinant of outcome. Medicine **86**:363–377.

10. **Murdoch DR, Corey GR, Hoen B, Miro JM, Fowler VG, Jr, Bayer AS, Karchmer AW, Olaison L, Pappas PA, Moreillon P, Chambers ST, Chu VH, Falco V, Holland DJ, Jones P, Klein JL, Raymond NJ, Read KM, Tripodi MF, Utili R, Wang A, Woods CW, Cabell CH.** 2009. Clinical presentation, etiology, and outcome of infective endocarditis in the 21st Century: the International Collaboration on Endocarditis-Prospective Cohort Study. Arch. Intern. Med. **169**:463–473.

11. **Paganelli FL, Willems RJ, Leavis HL.** 2012. Optimizing future treatment of enterococcal infections: attacking the biofilm? Trends Microbiol. **20**:40–49.

12. **Guiton PS, Hung CS, Hancock LE, Caparon MG, Hultgren SJ.** 2010. Enterococcal biofilm formation and virulence in an optimized murine model of foreign body-associated urinary tract infections. Infect. Immun. **78**:4166–4175.

13. **Frank KL, Barnes AM, Grindle SM, Manias DA, Schlievert PM, Dunny GM.** 2012. Use of recombinase-based *in vivo* expression technology to characterize *Enterococcus faecalis* gene expression during infection identifies *in vivo*-expressed antisense RNAs and implicates the protease Eep in pathogenesis. Infect. Immun. **80**:539–549.

14. **Nallapareddy SR, Singh KV, Sillanpää J, Zhao M, Murray BE.** 2011. Relative contributions of Ebp pili and the collagen adhesin Ace to host extracellular matrix protein adherence and experimental urinary tract infection by *Enterococcus faecalis* OG1RF. Infect. Immun. **79**:2901–2910.

15. **Singh KV, Nallapareddy SR, Sillanpää J, Murray BE.** 2010. Importance of the collagen adhesin Ace in pathogenesis and protection against *Enterococcus faecalis* experimental endocarditis. PLoS Pathog. **6**:e1000716. doi:10.1371/journal.ppat.1000716.

16. **Singh KV, Nallapareddy SR, Murray BE.** 2007. Importance of the *ebp* (endocarditis- and biofilm-associated pilus) locus in the pathogenesis of *Enterococcus faecalis* ascending urinary tract infection. J. Infect. Dis. **195**:1671–1677.

17. **Bourgogne A, Garsin DA, Qin X, Singh KV, Sillanpää J, Yerrapragada S, Ding Y, Dugan-Rocha S, Buhay C, Shen H, Chen G, Williams G, Muzny D, Maadani A, Fox KA, Gioia J, Chen L, Shang Y, Arias CA, Nallapareddy SR, Zhao M, Prakash VP, Chowdhury S, Jiang H, Gibbs RA, Murray BE, Highlander SK, Weinstock GM.** 2008. Large scale variation in *Enterococcus faecalis* illustrated by the genome analysis of strain OG1RF. Genome Biol. **9**:R110. doi:10.1186/gb-2008-9-7-r110.

18. **Paulsen IT, Banerjei L, Myers GS, Nelson KE, Seshadri R, Read TD, Fouts DE, Eisen JA, Gill SR, Heidelberg JF, Tettelin H, Dodson RJ, Umayam L, Brinkac L, Beanan M, Daugherty S, DeBoy RT, Durkin S, Kolonay J, Madupu R, Nelson W, Vamathevan J, Tran B, Upton J, Hansen T, Shetty J, Khouri H, Utterback T, Radune D, Ketchum KA, Dougherty BA, Fraser CM.** 2003. Role of mobile DNA in the evolution of vancomycin-resistant *Enterococcus faecalis*. Science **299**:2071–2074.

19. **Palmer KL, Godfrey P, Griggs A, Kos VN, Zucker J, Desjardins C, Cerqueira G, Gevers D, Walker S, Wortman J, Feldgarden M, Haas B, Birren B, Gilmore MS.** 2012. Comparative genomics of enterococci: variation in *Enterococcus faecalis*, clade structure in *E. faecium*, and defining characteristics of *E. gallinarum* and *E. casseliflavus*. mBio **3**:e00318–11. doi:10.1128/mBio.00318-11.

20. **Kristich CJ, Nguyen VT, Le T, Barnes AM, Grindle S, Dunny GM.** 2008. Development and use of an efficient system for random *mariner* transposon mutagenesis to identify novel genetic determinants of biofilm for-

mation in the core *Enterococcus faecalis* genome. Appl. Environ. Microbiol. **74**:3377–3386.

21. **Kemp KD, Singh KV, Nallapareddy SR, Murray BE.** 2007. Relative contributions of *Enterococcus faecalis* OG1RF sortase-encoding genes, *srtA* and *bps* (*srtC*), to biofilm formation and a murine model of urinary tract infection. Infect. Immun. **75**:5399–5404.

22. **Nallapareddy SR, Singh KV, Sillanpää J, Garsin DA, Hook M, Erlandsen SL, Murray BE.** 2006. Endocarditis and biofilm-associated pili of *Enterococcus faecalis*. J. Clin. Invest. **116**:2799–2807.

23. **Guiton PS, Hung CS, Kline KA, Roth R, Kau AL, Hayes E, Heuser J, Dodson KW, Caparon MG, Hultgren SJ.** 2009. Contribution of autolysin and sortase A during *Enterococcus faecalis* DNA-dependent biofilm development. Infect. Immun. **77**:3626–3638.

24. **Qin X, Singh KV, Xu Y, Weinstock GM, Murray BE.** 1998. Effect of disruption of a gene encoding an autolysin of *Enterococcus faecalis* OG1RF. Antimicrob. Agents Chemother. **42**:2883–2888.

25. **Ballering KS, Kristich CJ, Grindle SM, Oromendia A, Beattie DT, Dunny GM.** 2009. Functional genomics of *Enterococcus faecalis*: multiple novel genetic determinants for biofilm formation in the core genome. J. Bacteriol. **191**:2806–2814.

26. **Di Rosa R, Creti R, Venditti M, D'Amelio R, Arciola CR, Montanaro L, Baldassarri L.** 2006. Relationship between biofilm formation, the enterococcal surface protein (Esp) and gelatinase in clinical isolates of *Enterococcus faecalis* and *Enterococcus faecium*. FEMS Microbiol. Lett. **256**:145–150.

27. **Mohamed JA, Huang W, Nallapareddy SR, Teng F, Murray BE.** 2004. Influence of origin of isolates, especially endocarditis isolates, and various genes on biofilm formation by *Enterococcus faecalis*. Infect. Immun. **72**:3658–3663.

28. **Roggiani M, Schlievert PM.** 2000. Purification of streptococcal pyrogenic exotoxin A, p 59–66. *In* Evans TJ (ed), Septic shock methods and protocols, vol 36. Humana Press, Totowa, NJ.

29. **Dunny GM, Clewell DB.** 1975. Transmissible toxin (hemolysin) plasmid in *Streptococcus faecalis* and its mobilization of a noninfectious drug resistance plasmid. J. Bacteriol. **124**:784–790.

30. **Kristich CJ, Chandler JR, Dunny GM.** 2007. Development of a host-genotype-independent counterselectable marker and a high-frequency conjugative delivery system and their use in genetic analysis of *Enterococcus faecalis*. Plasmid **57**:131–144.

31. **Vesic D, Kristich CJ.** 15 February 2013. A Rex-family transcriptional repressor influences H_2O_2 accumulation by *Enterococcus faecalis*. J. Bacteriol. [Epub ahead of print.] doi:10.1128/JB.02135-12.

32. **Le Breton Y, Muller C, Auffray Y, Rince A.** 2007. New insights into the *Enterococcus faecalis* CroRS two-component system obtained using a differential-display random arbitrarily primed PCR approach. Appl. Environ. Microbiol. **73**:3738–3741.

33. **van der Vossen JM, van der Lelie D, Venema G.** 1987. Isolation and characterization of *Streptococcus cremoris* Wg2-specific promoters. Appl. Environ. Microbiol. **53**:2452–2457.

34. **Chuang ON, Schlievert PM, Wells CL, Manias DA, Tripp TJ, Dunny GM.** 2009. Multiple functional domains of *Enterococcus faecalis* aggregation substance Asc10 contribute to endocarditis virulence. Infect. Immun. **77**:539–548.

35. **Kristich CJ, Li YH, Cvitkovitch DG, Dunny GM.** 2004. Esp-independent biofilm formation by *Enterococcus faecalis*. J. Bacteriol. **186**:154–163.

36. **Heydorn A, Nielsen AT, Hentzer M, Sternberg C, Givskov M, Ersbøll BK, Molin S.** 2000. Quantification of biofilm structures by the novel computer program COMSTAT. Microbiology **146**:2395–2407.

37. **Vorregaard M.** 2008. COMSTAT2—a modern 3D image analysis environment for biofilms. Master's thesis. Technical University of Denmark (DTU), Kogens Lyngby, Denmark.

38. **Eleaume H, Jabbouri S.** 2004. Comparison of two standardisation methods in real-time quantitative RT-PCR to follow *Staphylococcus aureus* genes expression during in vitro growth. J. Microbiol. Methods **59**:363–370.

39. **Ballering KS.** 2010. Identification and characterization of novel genetic determinants of biofilm formation in *Enterococcus faecalis*. Ph.D. thesis. University of Minnesota, Minneapolis, MN.

40. **Bae T, Clerc-Bardin S, Dunny GM.** 2000. Analysis of expression of *prgX*, a key negative regulator of the transfer of the *Enterococcus faecalis* pheromone-inducible plasmid pCF10. J. Mol. Biol. **297**:861–875.

41. **Thomas VC, Hiromasa Y, Harms N, Thurlow L, Tomich J, Hancock LE.** 2009. A fratricidal mechanism is responsible for eDNA release and con-

tributes to biofilm development of *Enterococcus faecalis*. Mol. Microbiol. **72**:1022–1036.

42. **Ishikawa S, Kawai Y, Hiramatsu K, Kuwano M, Ogasawara N.** 2006. A new FtsZ-interacting protein, YlmF, complements the activity of FtsA during progression of cell division in *Bacillus subtilis*. Mol. Microbiol. **60**:1364–1380.

43. **Hamoen LW, Meile JC, de Jong W, Noirot P, Errington J.** 2006. SepF, a novel FtsZ-interacting protein required for a late step in cell division. Mol. Microbiol. **59**:989–999.

44. **Larsen R, Buist G, Kuipers OP, Kok J.** 2004. ArgR and AhrC are both required for regulation of arginine metabolism in *Lactococcus lactis*. J. Bacteriol. **186**:1147–1157.

45. **Kloosterman TG, Kuipers OP.** 2011. Regulation of arginine acquisition and virulence gene expression in the human pathogen *Streptococcus pneumoniae* by transcription regulators ArgR1 and AhrC. J. Biol. Chem. **286**: 44594–44605.

46. **Barcelona-Andres B, Marina A, Rubio V.** 2002. Gene structure, organization, expression, and potential regulatory mechanisms of arginine catabolism in *Enterococcus faecalis*. J. Bacteriol. **184**:6289–6300.

47. **Qin X, Singh KV, Weinstock GM, Murray BE.** 2001. Characterization of *fsr*, a regulator controlling expression of gelatinase and serine protease in *Enterococcus faecalis* OG1RF. J. Bacteriol. **183**:3372–3382.

48. **Donlan RM, Costerton JW.** 2002. Biofilms: survival mechanisms of clinically relevant microorganisms. Clin. Microbiol. Rev. **15**:167–193.

49. **Baldassarri L, Creti R, Arciola CR, Montanaro L, Venditti M, Di Rosa R.** 2004. Analysis of virulence factors in cases of enterococcal endocarditis. Clin. Microbiol. Infect. **10**:1006–1008.

50. **Konto-Ghiorghi Y, Mairey E, Mallet A, Dumenil G, Caliot E, Trieu-Cuot P, Dramsi S.** 2009. Dual role for pilus in adherence to epithelial cells and biofilm formation in *Streptococcus agalactiae*. PLoS Pathog. **5**:e1000422. doi:10.1371/journal.ppat.1000422.

51. **Chen SM, Tsai YS, Wu CM, Liao SK, Wu LC, Chang CS, Liu YH, Tsai PJ.** 2010. Streptococcal collagen-like surface protein 1 promotes adhesion to the respiratory epithelial cell. BMC Microbiol. **10**:320. doi:10.1186/1471-2180-10-320.

52. **Chuang-Smith ON, Wells CL, Henry-Stanley MJ, Dunny GM.** 2010. Acceleration of *Enterococcus faecalis* biofilm formation by aggregation substance expression in an *ex vivo* model of cardiac valve colonization. PLoS One **5**:e15798. doi:10.1371/journal.pone.0015798.

53. **Schlievert PM, Gahr PJ, Assimacopoulos AP, Dinges MM, Stoehr JA, Harmala JW, Hirt H, Dunny GM.** 1998. Aggregation and binding substances enhance pathogenicity in rabbit models of *Enterococcus faecalis* endocarditis. Infect. Immun. **66**:218–223.

54. **Trotter KM, Dunny GM.** 1990. Mutants of *Enterococcus faecalis* deficient as recipients in mating with donors carrying pheromone-inducible plasmids. Plasmid **24**:57–67.

55. **Bensing BA, Dunny GM.** 1993. Cloning and molecular analysis of genes affecting expression of binding substance, the recipient-encoded receptor(s) mediating mating aggregate formation in *Enterococcus faecalis*. J. Bacteriol. **175**:7421–7429.

56. **Barnes AM.** 2012. Ultrastructural characterization of matrix development and the role of extracellular DNA in early *Enterococcus faecalis* biofilms. Ph.D. thesis. The University of Minnesota, Minneapolis, MN.

57. **Thurlow LR, Thomas VC, Narayanan S, Olson S, Fleming SD, Hancock LE.** 2010. Gelatinase contributes to the pathogenesis of endocarditis caused by *Enterococcus faecalis*. Infect. Immun. **78**:4936–4943.

58. **Larsen R, van Hijum SA, Martinussen J, Kuipers OP, Kok J.** 2008. Transcriptome analysis of the *Lactococcus lactis* ArgR and AhrC regulons. Appl. Environ. Microbiol. **74**:4768–4771.

59. **Bourgogne A, Hilsenbeck SG, Dunny GM, Murray BE.** 2006. Comparison of OG1RF and an isogenic *fsrB* deletion mutant by transcriptional analysis: the Fsr system of *Enterococcus faecalis* is more than the activator of gelatinase and serine protease. J. Bacteriol. **188**:2875–2884.

60. **Dunny GM, Brown BL, Clewell DB.** 1978. Induced cell aggregation and mating in *Streptococcus faecalis*: evidence for a bacterial sex pheromone. Proc. Natl. Acad. Sci. U. S. A. **75**:3479–3483.